Brief Communication

Buoyancy-Induced Differences in Soot Morphology

JERRY C. KU

Mechanical Engineering Department, Wayne State University, 5050 Anthony Wayne Drive, Detroit, MI 48202

DEVON W. GRIFFIN* and PAUL S. GREENBERG

M / S 110-3, NASA Lewis Research Center, 21000 Brookpark Road, Cleveland, OH 44135

and

JOHN ROMA

Department of Electrical Engineering and Applied Physics, Case Western Reserve University, 10900 Euclid Avenue, Cleveland, OH 44106

INTRODUCTION

Reduction or elimination of buoyancy in flames affects the dominant mechanisms driving heat transfer, burning rates and flame shape. The absence of buoyancy produces longer residence times for soot formation, clustering and oxidation [1]. In addition, soot pathlines are strongly affected in microgravity [2]. We recently conducted the first experiments comparing soot morphology in normal and reduced-gravity laminar gas jet diffusion flames.

Thermophoretic sampling [3–5] is a relatively new but well-established technique for studying the morphology of soot primaries and aggregates. Although there have been some questions about biasing that may be induced due to sampling [6], recent analysis by Rosner et al. [7] showed that the sample is not biased when the system under study is operating in the continuum limit. Furthermore, even if the sampling is preferentially biased to larger aggregates, the size-invariant premise of fractal analysis should produce a correct fractal dimension [7].

EXPERIMENTAL PROCEDURES

The fuels were either propane or ethylene with flow rates of 1.0 and 1.5 cm^3/s injected into quiescent, atmospheric air from a nozzle with

* Corresponding author.

an inside diameter of 1.65 mm. The combustion chamber, cameras and supporting experimental hardware are in an experimental rig designed for use in the NASA Lewis Research Center's 2.2-s drop tower. As reported elsewhere, [2, 8], the luminous height of these flames in μG was 36 mm for ethylene at a flow rate of 1.0 cm^3/s with heights for the propane flame of 73 and 99 mm for flow rates of 1.0 and 1.5 cm^3/s, respectively. Normal gravity flame heights were 25 and 40 mm for the ethylene flames at flow rates of 1.0 and 1.5 cm^3/s. The respective values for propane were 45 and 65 mm, respectively. The propane values were averaged over the flicker heights. None of the normal gravity flames emitted soot but other work [2] indicates that the ethylene flames in microgravity did emit soot.

Individual probes were 3.3 mm wide and 0.05 mm thick with a slot 1.5 mm wide in the center, to which transmission electron microscope (TEM) grids were cemented. The grids were then inserted in the soot annulus, which was located via a newly-developed full-field imaging technique [9]. Multiple probes, each resident in the flame for approximately 35 ms, enabled simultaneous sampling of up to eight heights approximately 1.6 s after ignition in reduced gravity. This delay time was chosen to avoid both ignition transients and the effects of deceleration at the end of the drop.

Soot samples were photographed on the TEM and the negatives were digitized using a CCD camera in conjunction with a frame-grab-

bing board. With proper calibration, the diameter of primary particles d_p was determined as a function of height in the flame. Aggregates were measured for their maximum length, L_{max}, and width perpendicular to that length, W [10]. In addition to the dimensional measurement, projected areas were measured to enable a determination of the fractal dimension [4, 5, 10–12].

The fractal dimension is a measure of the geometrical structure of an object and provides information on the processes that formed the object. In the case of soot aggregates, the fractal dimension is indicative of the aggregation mechanism [10, 12]. To determine the fractal dimension of our aggregates, we used the previously suggested relationship [4]

$$N \sim \left[\frac{L_{max}}{d_p} \right]^{D_f}. \tag{1}$$

An accurate determination of the total dimension of primary particles present, N, is required to determine the fractal dimension. Modeling [13] and laboratory observation [5] indicate that for fractal aggregates, the number of primaries in the aggregate can be related to the projected area of the aggregate and the projected area of a primary by

$$N \equiv \left[\frac{A_a}{A_p} \right]^\alpha, \tag{2}$$

where A_a is the projected area of the aggregate, A_p the projected primary area, $\frac{\pi d_p^2}{4}$, with 1.08 as the accepted value for α [4, 5, 10]. This approximation attempts to correct for the overlap of primaries when a three-dimensional aggregate is projected onto two-dimensional film. The usual upper limit on this approximation is $N \leq 2500$ [4]. Recently, Köylü and Faeth [5] applied it when N was as large as approximately 18,000. With few exceptions, our aggregates had fewer than 18,000 primaries. The attendant uncertainties were calculated using standard linear regression methods [14].

RESULTS

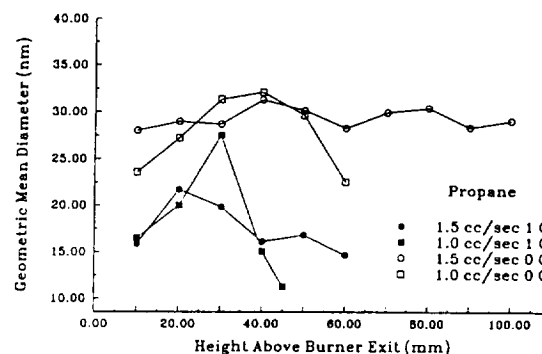Figures 1 and 2 illustrate the difference in primary size observed for propane and ethy-

Fig. 1. Geometric mean diameter as a function of height above burner exit: propane flames.

lene gas jets respectively, as a function of height above the burner for different flow rates and gravitational levels. A minimum of 80 primaries were measured for each datum. The typical geometric standard deviation to a 95% confidence level is approximately 10 nm. This uncertainty, larger than often reported, was due to the observed wide variations in primary size within individual aggregates.

The larger size of μG primaries can be explained by the computationally predicted longer residence times, which are approximately a factor of 20 larger. Additionally, the soot formation, growth and burnout processes as evidence by primary size are clearly shown in 1G, whereas this trend is only fully observed for the 1.5 cm^3/s propane flame in μG. For example, the burnout process may be missing in both 1.5 cm^3/s flames in reduced gravity.

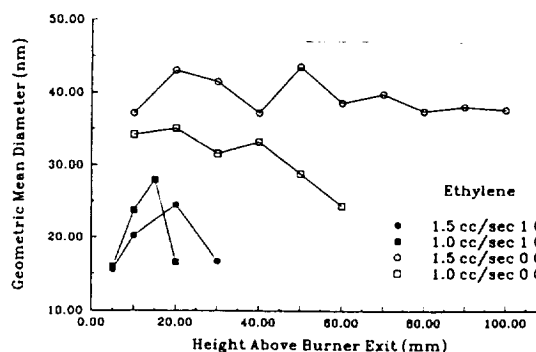Table 1 presents mean aggregate properties for two specific cases. For ethylene, aggregate

Fig. 2. Geometric mean diameter as a function of height above burner exit: ethylene flames.

TABLE 1

Buoyancy-Induced Differences in Soot Morphology J. C. Ku *et al.*

Fuel	Flow Rate (cm³/s)	Gravity Level	Mean Aggregate Length (μm)	95% Bound (μm)	Actual Min/Max (μm)	Height Above Burner (mm)	Fractal Dimension	Aggregate Number Analyzed
Ethylene	1.0	1 G	0.21	0.10 → 0.42	0.11 → 0.52	10	1.41 ± 0.10	47
Ethylene	1.0	0 G	4.71	1.12 → 19.8	1.14 → 18.53	10	1.93 ± 0.34	19
Propane	1.5	1 G	0.27	0.14 → 0.50	0.14 → 0.54	30	1.71 ± 0.13	40
Propane	1.5	0 G	1.53	0.48 → 4.89	0.50 → 7.27	50	1.57 ± 0.07	39

Burner Diameter: 1.65 mm

properties were measured at a height above the burner of 10 mm (HAB). While these data are preliminary due to the limited number of tests, several trends appear noteworthy. The aggregates generated in 1G were short and nearly linear, as the fractal dimension indicates. On the other hand, μG aggregates were not only larger overall but had a more two-dimensional structure, as indicated by their fractal dimension.

For propane at a mass flow rate of 1.5 cm³/s, the 1G flame was sampled at a height of 30 mm and the 0 G at 50 mm; these heights corresponded approximately to the half-height of the luminous flame. The fractal dimension for propane in 1G matches that previously reported [4, 5], whereas that for ethylene does not. However, the latter discrepancy may be understood by noting the low sampling height, which may indicate that cluster-cluster aggregation has just begun.

REFERENCES

1. Mortazavi, S., Sunderland, P. B., Jurn, J., Köylü, Ü. Ö., and Faeth, G. M., AIAA Paper No. 93-078, 1993.
2. Sunderland, P. B., Mortazavi, S., Faeth, G. M., and Urban, D. L., *Combust. Flame* 96:97-103 (1994).
3. Dobbins, R. A., and Megaridis, C. M., *Langmuir* 3:254-259 (1987).
4. Megaridis, C. M., and Dobbins, R. A., *Combust. Sci. Technol.* 71:95-109 (1990).
5. Köylü, Ü. Ö., Faeth, G. M., *Combust. Flame* 89:140-156 (1992).
6. Griffin, D. W., and Greenberg, P. S., Second International Microgravity Combustion Workshop, NASA Conference Publication 10113, 1992.
7. Rosner, D. E., Mackowski, D. W., and Garcia-Ybarra, P., *Combust. Sci. Technol.* 80:87-101 (1991).
8. Bahadori, Y. M., Edelman, R. B. Stocker, D. P., and Olson, S. L., *AIAA J.* 28:236-244 (1990).
9. Greenberg, P. S., Ku. J. C., Lin, K.-C., Köylü, Ü. Ö., and Faeth, G. M., in preparation.
10. Samson, R. J., Mulholland, G. W., and Gentry, J. W., *Langmuir* 3:272-281 (1987).
11. Tence, M., Chevalier, J. P., and Jullien, R., *J. Phys. (Paris)* 47:1989-1998 (1986).
12. Jullien, R., and Botet, R., *Aggregation and Fractal Aggregates*, World Scientific Publishing, Singapore, 1987.
13. Meakin, P., Donn, B. and Mulholland, G. W., *Langmuir* 5:510-518 (1989).
14. Taylor, J. R., *An Introduction to Error Analysis*, University Science Books, Mill Valley, CA, 1982.